Nickel Dithiolenes Revisited: Structures and Electron Distribution from Density Functional Theory for the Three-Member Electron-Transfer Series $[Ni(S_2C_2Me_2)_2]^{0,1-,2-}$

Booyong S. Lim, Dmitry V. Fomitchev, and R. H. Holm*

Department of Chemistry and Chemical Biology, Harvard University, Cambridge, Massachusetts 02138

Received February 1, 2001

The complexes $[Ni(S_2C_2Me_2)_2]^z$ ($z = 0, 1-, 2-$) have been isolated for the purpose of investigating their electronic structures in a reversible three-member electron-transfer series. Members are interrelated by reversible redox reactions with $E_{1/2}(0/1-) = -0.15$ V and $E_{1/2}(1-/2-) = -1.05$ V versus SCE in acetonitrile. The three complexes have nearly planar structures of idealized D_{2h} symmetry. As the series is traversed in the reducing direction, Ni−S and C−S bond lengths increase; the chelate ring C−C bond length decreases from the neutral complex to the monoanion and does not change significantly in the dianion. Structural trends are compared with previous results for $[Ni(S_2C_2R_2)_2]^{1-,2-}$. Following the geometrical changes, values of ν_{Ni-S} and ν_{C-S} decrease, while the value of ν_{C-C} increases with increased reduction. Geometry optimizations at the density functional theory (DFT) level were performed for all members of the series. Geometrical parameters obtained from the calculations are in good agreement with the experimental findings. The $5b_{2g}$ orbital was identified as the LUMO in $[Ni(S_2C_2Me_2)_2]$, the SOMO in $[Ni(S_2C_2Me_2)_2]^{1-}$, and the HOMO in $[Ni(S_2C_2Me_2)_2]^{2-}$. Unlike in the situation in the $[M(CO)_2(S_2C_2Me_2)_2]^z$ series (M = Mo, W; $z = 0, 1-, 2-$), the apparent contribution from the metal d orbital in the electroactive orbital is not constant. In the present series, the d_{xz} contribution increases from 13 to 20 to 39% upon passing from the neutral to the monoanionic to the dianionic complex. Accurate calculation of EPR *g*-values of $[Ni(S_2C_2Me_2)_2]^{1-}$ by DFT serves as a test for the reliability of the electronic structure calculations.

Introduction

The most characteristic feature of transition metal dithiolene complexes derived from d^{1-9} metals is the existence of electron-transfer series whose members are interrelated by reversible one-electron steps.[1−4] Initial developments in the dithiolene field, which have been summarized by McCleverty,[1] led to the recognition and experimental realization of the planar three-member series **1**

Series **1**

$$[M(S_2C_2R_2)_2] \leftrightarrow [M(S_2C_2R_2)_2]^{1-} \leftrightarrow [M(S_2C_2R_2)_2]^{2-}$$

with M = Ni, Pd, or Pt in which the terminal members are diamagnetic and the monoanion has an $S = {}^1/_2$ ground state. Mono- and dication members of a five-member series are conjecturable, with the latter involving M^{II} bound to two ligands in the 1,2-dithione form. However, no species of the types $[M(S_2C_2R_2)_2]^{1+,2+}$ have been detected (excluding species with $R = NR'_2$). The well-known ambiguities in limiting descriptions of metal and ligand oxidation states are summarized in Figure

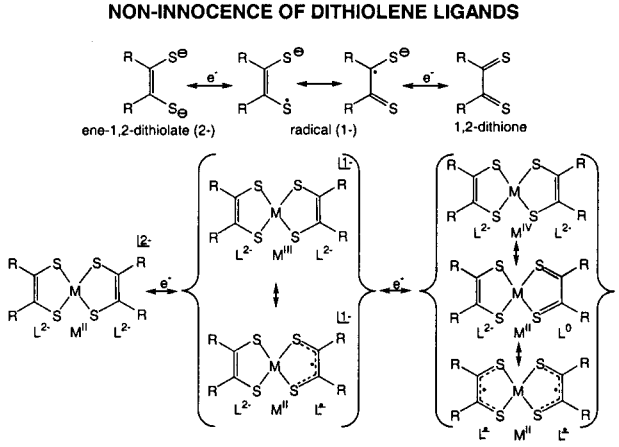

Figure 1. The three oxidation levels of a dithiolene ligand and depictions of the limiting ligand and metal oxidation levels for planar members of the electron-transfer series $[M(S_2C_2R_2)_2]^{0,1-,2-}$.

1. While the structural and electronic properties of dianions are sensibly consistent with the indicated M^{II}-enedithiolate description, two and three formulations are conceivable for the monoanion and neutral complex, respectively. For the latter, one of these is a ligand diradical whose spins are antiferromagnetically coupled to be consistent with diamagnetism. Numerous members of series **1**, especially with M = Ni, have been isolated and/or generated in solution by chemical or electrochemical reactions. Because redox potentials are markedly dependent on the nature of the R substituent, certain members of a given series have not been isolated in substance. For example, the complexes $[Ni(S_2C_2(CN)_2)_2]^{2-,1-}$ were isolated in early investigations.[5,6] Reversible chemical oxidation to the neutral complex has not been achieved and would require strongly positive potentials

(1) McCleverty, J. A. *Prog. Inorg. Chem.* **1968**, *10*, 49−221.
(2) Hoyer, E.; Dietzsch, W.; Schroth, W. *Z. Chem.* **1971**, *11*, 41−53.
(3) Mahadevan, C. *J. Crystallogr. Spectrosc. Res.* **1986**, *16*, 347−416.
(4) Olk, R.-M.; Olk, B.; Dietzsch, W.; Kirmse, R.; Hoyer, E. *Coord. Chem. Rev.* **1992**, *117*, 99−131.
(5) Davison, A.; Edelstein, N.; Holm, R. H.; Maki, A. H. *Inorg. Chem.* **1963**, *2*, 1227−1232.
(6) Billig, E.; Williams, R.; Bernal, I.; Waters, J. H.; Gray, H. B. *Inorg. Chem.* **1964**, *3*, 663−666.
(7) Schrauzer, G. N.; Mayweg, V. P. *J. Am. Chem. Soc.* **1965**, *87*, 3585−3592.
(8) Hoyer, E.; Dietzsch, W.; Schroth, W. *Chem. Ber.* **1969**, *102*, 603−614.
(9) Browall, K. W.; Interrante, L. V. *J. Coord. Chem.* **1973**, *3*, 27−38.

10.1021/ic010138y CCC: $20.00
Published on Web 07/10/2001

Table 1. Crystallographic Data[a] for Compounds Containing $[Ni(S_2C_2Me_2)_2]^z$ with $z = 0$, 1−, or 2−

	$[Ni(S_2C_2Me_2)_2]$	$(Et_4N)[Ni(S_2C_2Me_2)_2]$	$(Et_4N)_2[Ni(S_2C_2Me_2)_2]$
formula	$C_8H_{12}NiS_4$	$C_{16}H_{32}NNiS_4$	$C_{24}H_{52}N_2NiS_4$
fw	295.13	425.38	555.63
cryst syst	triclinic	monoclinic	triclinic
space group	*P*1	*C*2/*c*	*P*1
Z	1	4	5
a, Å	7.038(1)	13.107(1)	8.9920(7)
b, Å	7.124(1)	12.321(1)	18.905(2)
c, Å	7.415(1)	13.175(1)	24.503(2)
α, deg	114.702(1)		109.155(2)
β, deg	117.385(2)	101.085(2)	94.881(2)
γ, deg	92.287(2)		101.874(1)
V, Å^3	287.27(7)	2088.1(3)	3797.7(5)
d_{calc}, g/cm^3	1.706	1.353	1.215
μ, mm^{-1}	2.366	1.326	0.928
θ range, deg	3.29−22.47	2.29−22.50	1.18−27.74
GOF (F^2)	1.150	1.103	1.004
R1[b] (wR2[c]), %	3.60(11.12)	3.74(9.21)	3.62(8.64)

[a] Obtained with graphite-monochromatized Mo Kα ($\lambda = 0.710\,73$ Å) radiation. [b] $R1 = \sum||F_o| - |F_c||/\sum|F_o|$. [c] $wR2 = \{\sum[w(F_o^2 - F_c^2)^2]/\sum[w(F_o^2)^2]\}^{1/2}$.

(≥1 V vs SCE).[1] In other cases such as $[Ni(S_2C_2H_2)_2]^z$, the $z = 0,1-$ species have been isolated,[7−9] but the fully reduced member has not, although it is within an easy potential range ($E_{1/2}(1-/2-) \approx -0.9$ V).[1,8]

There are three examples of series **1** in which the three members have been isolated: (**a**) $[Ni(S_2C_2(CF_3)_2)_2]^{0,1-,2-}$,[5,10,11] (**b**) $[Ni(S_2C_2Ph_2)_2]^{0,1-,2-}$,[5,12] and (**c**) $[Ni(3,5\text{-}Bu^t_2bdt)_2]^{0,1-,2-}$ (bdt = benzene-1,2-dithiolate(2−)).[13] In series **1a**, the structures of the $z = 0$, or 1− members are known.[14−16] The same is true of series **1b**.[17−19] Structures are available for all members of series **1c**.[13] We have become interested in series **1d**, $[Ni(S_2C_2Me_2)_2]^{0,1-,2-}$, in part because of the utility of the $z = 0$ species in the synthesis of bis(dithiolene)molybdenum[20] and -tungsten[21] complexes, and also because the simplicity of the ligand system lends the series to theoretical investigation. The neutral complex has been previously prepared,[12] and the mono- and dianions have been generated in solution[7,22] but not isolated. In this investigation, we have prepared the three members of series **1d**, determined their crystal structures, and examined their electronic structures by means of density functional theory. This is the first bis(dithiolene) series in which complexes have been isolated, structures determined, and contemporary theoretical calculations carried out for three oxidation levels.

Experimental Section

Preparation of Compounds. All reactions and manipulations were conducted under a pure dinitrogen atmosphere using either an inert atmosphere box or standard Schlenk techniques. Acetonitrile, ether, and THF were dried using the Innovative Technology solvent purification system and stored over 4-Å molecular sieves. In the following preparations, all volume reduction and evaporation steps were performed in vacuo.

$[Ni(S_2C_2Me_2)_2]$. This compound was obtained by a published method[12] and was recrystallized from toluene. Absorption spectrum (THF) λ_{max}, nm (ϵ_M): 277 (26 300), 300 (29 100), 405 (sh, 1530), 571 (1680), 771 (21 500). This spectrum is consistent with that reported.[12]

$(Et_4N)[Ni(S_2C_2Me_2)_2]$. A solution of 51 mg (0.35 mmol) of $(Et_4N)(BH_4)$ was added to a blue-violet solution of 105 mg (0.36 mmol) of $[Ni(S_2C_2Me_2)_2]$ in 2 mL of THF. The reaction mixture was stirred for 3 h to generate a red-violet solution. The solvent was removed, and the solid residue was dissolved in a minimal volume of acetonitrile. The solution was filtered, and several volume equivalents of ether were layered upon the filtrate. The mixture was allowed to stand overnight. The product was obtained as 80 mg (54%) of black, needlelike crystals. Absorption spectrum (acetonitrile) λ_{max}, nm (ϵ_M): 310 (13 100), 357 (4050), 523 (1490), 632 (sh, 364), 932 (9710). Anal. Calcd for $C_{16}H_{32}NNiS_4$: C, 45.18; H, 7.58; N, 3.29; S, 30.15. Found: C, 45.08; H, 7.51; N, 3.32; S, 30.08.

$(Et_4N)_2[Ni(S_2C_2Me_2)_2]$. Sodium (10 mg, 0.43 mmol) was added to a solution of 80 mg (0.45 mmol) of anthracene in 2 mL of THF. The dark blue solution was stirred for 6 h and filtered. The filtrate was added dropwise to a solution of 66 mg (0.22 mmol) of $[Ni(S_2C_2Me_2)_2]$ in 2 mL of THF. As the reaction proceeded, the reaction mixture became dark brown, at which point it was stirred for 1 h. A solution of 74 mg (0.45 mmol) of Et_4NCl in 1 mL of acetonitrile was added. The mixture was stirred for 10 min and reduced to dryness. The residue was washed with ether (3 × 3 mL) and dissolved in a minimal volume of acetonitrile to give an orange-brown solution. The solution was filtered, and several volume equivalents of ether were introduced in the filtrate by vapor diffusion. The product was isolated as 60 mg (50%) of orange-brown, blocklike crystals. Absorption spectrum (acetonitrile) λ_{max}, nm (ϵ_M): 280 (sh, 19 400), 320 (sh, 12 700), 392 (sh, 1370), 530 (sh, 200). Anal. Calcd for $C_{24}H_{52}N_2NiS_4$: C, 51.88; H, 9.43; N, 5.04; S, 23.08. Found: C, 51.75; H, 9.51; N, 4.96; S, 23.15.

X-ray Structure Determinations. Structures of the three compounds in Table 1 were determined. Suitable crystals of $[Ni(S_2C_2Me_2)_2]$ were obtained from a solution in THF/hexanes, and crystals of $(Et_4N)[Ni(S_2C_2Me_2)_2]$ and $(Et_4N)_2[Ni(S_2C_2Me_2)_2]$ were obtained by vapor diffusion of ether into acetonitrile solutions. Crystals were mounted on glass fibers in paratone-N oil and cooled in a stream of dinitrogen (−60 °C). Diffraction data were collected with a Siemens (Bruker) SMART CCD area detector system, using ω-scans of 0.3°/frame. In all cases, a complete hemisphere of data was collected. Cell parameters were determined using SMART software. The SAINT package was used for integration of data, Lorentz polarization and decay corrections, and merging of the data. Absorption corrections were applied with SADABS. All structures were solved with direct methods. Space groups

(10) Davison, A.; Edelstein, N.; Holm, R. H.; Maki, A. H. *J. Am. Chem. Soc.* **1963**, *85*, 2029−2030.
(11) Davison, A.; Edelstein, N.; Holm, R. H.; Maki, A. H. *Inorg. Chem.* **1964**, *3*, 814−823.
(12) Schrauzer, G. N.; Mayweg, V. P. *J. Am. Chem. Soc.* **1965**, *87*, 1483−1489.
(13) Sellman, D.; Binder, H.; Häussinger, D.; Heinemann, F. W.; Sutter, J. *Inorg. Chim. Acta* **2000**, *300*−*302*, 829−836.
(14) Schmitt, R. D.; Wing, R. M.; Maki, A. H. *J. Am. Chem. Soc.* **1968**, *91*, 4394−4401.
(15) Wing, R. M.; Schlupp, R. L. *Inorg. Chem.* **1970**, *9*, 471−475.
(16) Miller, J. S.; Calabrese, J. C.; Epstein, A. J. *Inorg. Chem.* **1989**, *28*, 4230−4238.
(17) Sartain, D.; Truter, M. R. *J. Chem. Soc. A* **1967**, 1264−1272.
(18) Mahadevan, C.; Seshasayee, M.; Kuppusamy, P.; Manoharan, P. T. *J. Crystallogr. Spectrosc. Res.* **1984**, *14*, 179−191.
(19) Megnamisi-Belombe, M.; Nuber, B. *Bull. Chem. Soc. Jpn.* **1989**, *62*, 4092−4094.
(20) Lim, B. S.; Donahue, J. P.; Holm, R. H. *Inorg. Chem.* **2000**, *39*, 263−273.
(21) Sung, K.-M.; Holm, R. H. *Inorg. Chem.* **2000**, *39*, 1275−1281.
(22) Kirmse, R.; Möller, E.; Seitz, C.; Reinhold, J. *Z. Anorg. Allg. Chem.* **2000**, *623*, 159−168.

Table 2. Selected Mean Bond Lengths (Å) and Angles (deg) from X-ray Data and Optimized Geometrical Parameters for the Complexes $[Ni(S_2C_2Me_2)_2]^z$ with $z = 0$, 1−, or 2−

	X-ray data			optimized parameters		
	$z = 0$	$z = 1-$	$z = 2-$[a]	$z = 0$	$z = 1-$	$z = 2-$
Ni−S	2.128(1)	2.143(1)	2.179(4)[c]	2.137	2.165	2.209
C−S	1.714(1)	1.737(4)	1.761(4)[d]	1.704	1.732	1.757
C−C	1.365(9)	1.342(6)	1.337(7)[e]	1.377	1.356	1.347
C−C(CH_3)	1.515(6)	1.512(4)	1.508(9)	1.492	1.497	1.499
S−Ni−S[b]	91.35(6)	90.64(4)	90.1(2)	90.76	90.52	89.81

[a] Mean values. [b] Bite angle of the chelate rings. [c] Range of 10, 2.1744(7)−2.1884(8). [d] Range of 10, 1.754(3)−1.769(2). [e] Range of 5, 1.329(4)−1.345(4).

were assigned by analysis of symmetry and observed systematic absences determined by XPREP and by successful refinement of the structure. Any missing symmetry elements were checked with PLATON. Structures were refined by a full-matrix least-squares method against F^2, with statistical weighting and anisotropic displacement parameters for all non-hydrogen atoms. In the final stages of refinement, hydrogen atoms were added at idealized positions and refined as riding atoms with a uniform value of U_{iso}. All least-squares refinements were done with the SHELXL-97 structure refinement package.

The asymmetric units contain one-half ($[Ni(S_2C_2Me_2)_2]$), (Et_4N)[Ni($S_2C_2Me_2)_2$]) or two and one-half (($(Et_4N)_2[Ni(S_2C_2Me_2)_2]$) formula weights. The ethyl groups of the cation in (Et_4N)$[Ni(S_2C_2Me_2)_2]$ were disordered over two positions and were refined accordingly. Crystal data and final agreement factors are listed in Table 1. Selected bond lengths and angles are given in Table 2. (See paragraph at the end of this article for Supporting Information available.)

Other Physical Measurements. All measurements were made under anaerobic conditions. Absorption spectra were determined with a Cary 50 Bio spectrophotometer. The spectrum of $[Ni(S_2C_2Me_2)_2]^{1-}$ in the near-IR region was taken with a Varian 2390 UV−vis−NIR spectrophotometer. IR spectra were measured with a Nicolet Nexus 470 FT-IR spectrometer. Electrochemical measurements were performed with a PAR Model 263 potentiostat/galvanostat using a platinum working electrode and 0.1 M (Bu_4N)(PF_6) supporting electrolyte. Potentials are referenced to the SCE. EPR spectra were recorded on a Bruker ESP 300 spectrometer in dichloromethane/DMF (1:1 v/v) at 77 K.

Computational Details. All theoretical calculations are based on approximate density functional theory (DFT)[23,24] and were performed using the Amsterdam Density Functional (ADF) package.[25] In the coordinate system employed, the molecule is in the *xy*-plane, the *x*-axis bisects the chelate ring, and the *y*-axis bisects the S−Ni−S angle external to the chelate rings. Basis functions and fit functions for nickel, sulfur, carbon, and hydrogen atoms were used as provided from database IV of the ADF package. This includes Slater-type orbital (STO) triple-ζ all-electron basis sets for nickel, sulfur, carbon, and hydrogen atoms and a single polarization function for the latter three atoms. Relativistic effects have been accounted for by the quasi-relativistic treatment, which employs the first-order Pauli Hamiltonian. Noting the caution expressed by te Velde et al.[26] in using the all-electron basis set in conjunction with the quasi-relativistic method based on the Pauli Hamiltonian, we have tested basis sets employing the frozen core approximation and corrected for relativistic effects either by the Pauli formalism or by zero-order regular approximation (ZORA). Although the composition, symmetry, and energy separations of the frontier orbitals of [Ni($S_2C_2Me_2)_2]^{0,1-,2-}$ were nearly the same as in the case of the all-electron basis set, calculated bond lengths and components of the **g**-tensor of $[Ni(S_2C_2Me_2)_2]^{1-}$ were in less satisfactory agreement with the experimental data. These results are not reported here. All geometry optimizations are spin-restricted and based on the local density approximations in the parametrization of Vosko, Wilk, and Nusair.[27] Gradient corrections for exchange (Becke[28]) and correlation (Lee−Yang−Parr[29]) effects were applied self-consistently. Geometry optimizations are based on a quasi-Newton approach;[30] starting geometrical parameters were taken from the X-ray structures. Vibrational analyses were carried out for all optimized geometries to ensure that they are true stationary points on the potential energy surface. EPR **g**-tensors were computed for optimized structures using an algorithm implemented in ADF,[31] version 1999.02.

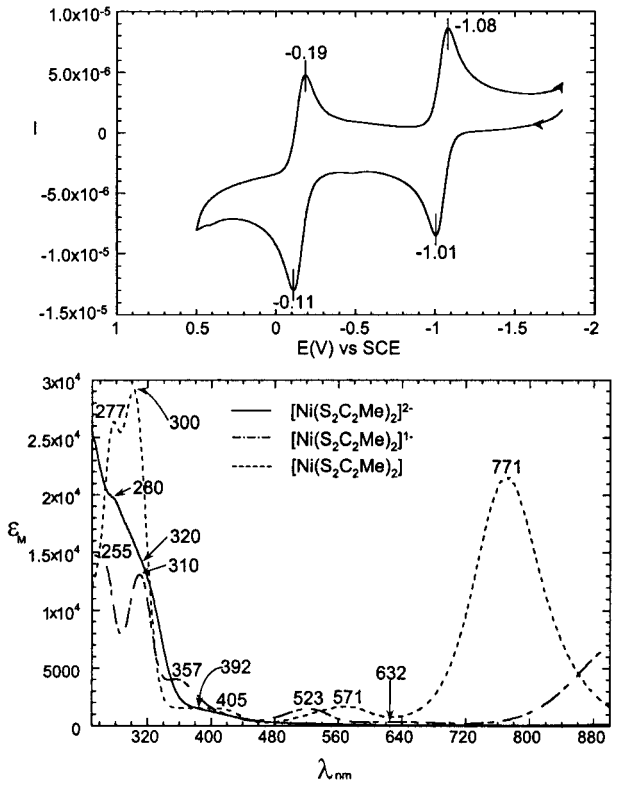

Figure 2. Upper: Cyclic voltammogram (100 mV/s) of $[Ni(S_2C_2Me_2)_2]^{2-}$ in acetonitrile; peak potentials vs SCE are indicated. Lower: Absorption spectra of the series $[Ni(S_2C_2Me_2)_2]^{0,1-,2-}$ in acetonitrile in the 250−900 nm interval. The absorption band of the monoanion at 932 nm is not shown.

Results and Discussion

Synthesis. The original report of series **1** based on [Ni($S_2C_2Me_2)_2]$[31] is confirmed by the cyclic voltammogram in Figure 2 of $[Ni(S_2C_2Me_2)_2]^{2-}$, from which we obtain the values of $E_{1/2}(1-/2-) = -1.05$ V and $E_{1/2}(0/1-) = -0.15$ V in acetonitrile. Attempted oxidation of the neutral complex yielded poorly defined irreversible waves. The monoanion and dianion are readily prepared by reduction of the neutral complex in THF. (Et_4N)$[Ni(S_2C_2Me_2)_2]$ was obtained by reduction with borohydride and isolated as black crystals (54%). Reduction with sodium anthracenide yielded $(Et_4N)_2[Ni(S_2C_2Me_2)_2]$ as orange-

(23) Parr, R. G.; Yang, W. *Density Functional Theory of Atoms and Molecules*; Oxford University Press: Oxford, 1989.
(24) Ziegler, T. *Chem. Rev.* **1991**, *91*, 651−677.
(25) *The Amsterdam Density Functional Program Package*, v. 1999.02; Theoretical Chemistry Group of the Vrije Universiteit in Amsterdam and Theoretical Chemistry Group of the University of Calgary, Canada, with significant contributions from academic collaborators elsewhere. Baerends, E. J.; Ellis, D. E.; Ros, P. *Chem. Phys.* **1973**, *2*, 41. Versluis, L.; Ziegler, T. *J. Chem. Phys.* **1988**, *88*, 322. te Velde, G.; Baerends, E. J. *Comput. Phys.* **1992**, *99*, 84. Fonseca Guerra, C.; Snijders, J. G.; te Velde, G.; Baerends, E. J. *Theor. Chim. Acta* **1998**, *99*, 391.
(26) teVelde, G.; Bickelhaupt, F.; Baerends, E. J.; Fonseca Guerra, C.; Van Gisbergen, S. J. A.; Snijders, J. G.; Ziegler, T. *J. Comput. Chem.* **2001**, *22*, 931−967.
(27) Vosko, S. H.; Wilk, L.; Nusair, M. *Can. J. Phys.* **1980**, *58*, 1200−1211.
(28) Becke, A. D. *Phys. Rev. A* **1988**, *38*, 3098−3100.
(29) Lee, C.; Yang, W.; Parr, R. G. *Phys. Rev. B* **1988**, *37*, 785−789.
(30) Fan, L.; Ziegler, T. *J. Chem. Phys.* **1991**, *95*, 7401−7408.
(31) van Lenthe, E.; Wormer, P. E. S.; van der Avoird, A. *J. Chem. Phys.* **1997**, *107*, 2488−2498.

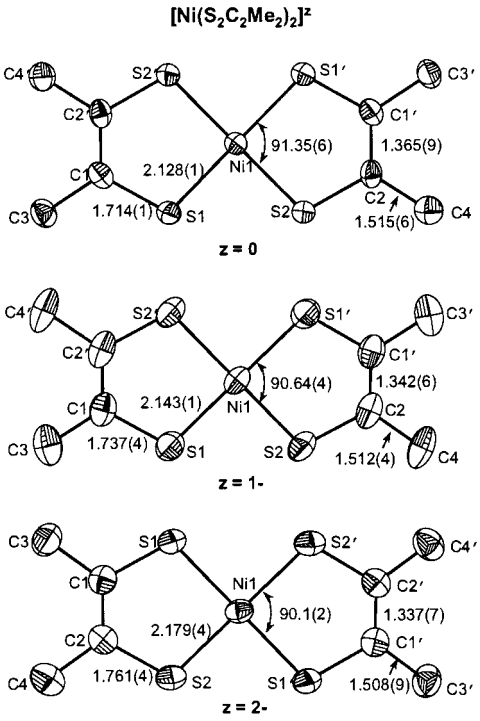

Figure 3. Structures of members of the electron-transfer series $[Ni(S_2C_2Me_2)_2]^{0,1-,2-}$ with atom labeling schemes and 50% probability ellipsoids. Primed and unprimed atoms are related by inversion symmetry. Except for the C1′−C2 distances in $z = 0$ and 1−, bond lengths are mean values.

brown crystals (50%). Absorption spectra reveal the intense low energy bands characteristic of the neutral and monoanion members of series **1**. In THF, the band for $[Ni(S_2C_2Me_2)_2]$ occurs at 771 nm (Figure 2) and for $[Ni(S_2C_2Me_2)_2]^{1-}$ at 932 nm in acetonitrile (not shown). A corresponding feature is absent in the spectrum of $[Ni(S_2C_2Me_2)_2]^{2-}$, whose lowest energy absorption detected is a probable d−d band near 530 nm.

Structural Trends. Structures of the three complexes are set out in Figure 3. All are planar or nearly so with imposed centrosymmetry. Certain trends in bond lengths are evident from the data in Table 2. As electrons are added, the Ni−S and C−S distances increase. The chelate ring C−C distance decreases upon passing from the neutral complex to the monoanion but does not change significantly upon further reduction to the dianion. Among structures of $[Ni(S_2C_2R_2)_2]^{0,1-}$ complexes with the same chelate ring substituent, a similar trend is evident with R = Ph[17−19] but is not clear with R = CF_3.[14−16,33] In the latter case, intrinsic bond length differences may be affected by cation−anion stacking in crystals of charge-transfer complexes and by the accuracy of the structure determination. Mean bond lengths of anions in $(Bu_4N)[Ni(S_2C_2Ph_2)_2]$[18] and $(Cp^*_2Fe)[Ni(S_2C_2(CF_3))_2]$[16] are, however, in close agreement with each other and with those in $[Ni(S_2C_2Me_2)_2]^{1-}$. Any previous assessment of monoanion−dianion structural trends has been restricted to $[Ni(S_2C_2(CN)_2)_2]^{1-,2-}$ because of the stability of the dianion afforded by the electronegative ring substituent. Examination of data from the more recent and accurate structures of the monoanion[34−38] and dianion[34,39−42] indicates that the bond length trends in Table 2 are followed with few exceptions. Indeed, the trend is evident from the first comparative determination of anion structures. In $(Et_4N)[Ni(S_2C_2(CN)_2)_2]$, mean bond lengths are Ni−S = 2.149(2) Å, C−S = 1.72(1) Å, and C−C = 1.37(1) Å, and in $(Bu_4N)_2[Ni(S_2C_2(CN)_2)_2]$, the values are Ni−S = 2.175(2) Å, C−S = 1.729(5) Å, and C−C = 1.360(7) Å.[34] Although comparisons are imprecise because of differences in crystal environment, temperature, and accuracy, the collective results indicate an increase in Ni−S distances by ∼0.02 Å, an increase in C−S distances by ≤0.02 Å, or no change or a very slight decrease in C−C distances. In the series $[Ni(3,5\text{-}Bu^t_2\text{-}bdt)_2]^{0,1-,2-}$,[13] the same trends in Ni−S and C−S bond lengths occur, except that the chelate ring C−C distance is invariant in the *o*-phenylene ligand backbone. As series **1** (M = Ni) is traversed in the reducing direction, the bond length changes indicate that the added charge is delocalized and that in the dianion the ligand approaches the classical enedithiolate oxidation level. Bond lengths in $[Ni(S_2C_2Me_2)_2]^{2-}$ are in close agreement with the typical distances S−C(sp^2) = 1.751(17) Å and (sp^2)C=C(sp^2) = 1.331(9) Å; for comparison, S=C(sp^2) = 1.671(24) Å.[43] Because there is adequate evidence from this work and from the investigations cited that the structural trends in Table 2 are intrinsic to the series $[Ni(S_2C_2R_2)_2]^{0,1-,2-}$, we have undertaken an analysis of electronic structure using the results of density functional theory calculations. Previous theoretical investigations have ranged from early to more advanced extended Hückel calculations,[7,44,45] Xα[46] and INDO-type analyses,[47] and DFT treatments for neutral and monoanionic complexes[48−51] including $[Ni(S_2C_2(CN)_2)_2]^{1-}$[48] and $[M(S_2C_2H_2)_2]$ (M = Ni, Pd, Pt).[50,51]

DFT Results. Full geometry optimizations for the complexes $[Ni(S_2C_2Me_2)_2]^{0,1-,2-}$ in D_{2h} symmetry were performed. The results for four bond lengths and the S−Ni−S chelate ring angle are included in Table 2. The largest discrepancy in bond distance is 0.032 Å in the Ni−S distance of the dianion, and the largest

(32) Olson, D. C.; Mayweg, V. P.; Schrauzer, G. N. *J. Am. Chem. Soc.* **1966**, *88*, 4876−4882.
(33) Singhabhandhu, A.; Robinson, P. D.; Fang, J. H.; Geiger, W. E., Jr. *Inorg. Chem.* **1975**, *14*, 318−323.
(34) Kobayashi, A.; Sasaki, Y. *Bull. Chem. Soc. Jpn.* **1977**, *50*, 2650−2657.
(35) Clemenson, P. I.; Underhill, A. E.; Hursthouse, M. B.; Short, R. L. *J. Chem. Soc., Dalton Trans.* **1988**, 1689−1691.
(36) Lemke, M.; Knoch, F.; Kisch, H.; Salbeck, J. *Chem. Ber.* **1995**, *128*, 131−136.
(37) Day, M. W.; Qin, J.; Yang, C. *Acta Crystallogr.* **2000**, *C54*, 1413−1414.
(38) Long, D.-L.; Cui, C.-P.; Hu, H.-M.; Chen, J.-T.; Ji, Z.-P.; Zhang, Y.-D.; Huang, J.-S. *Inorg. Chim. Acta* **1999**, *293*, 89−94.
(39) Clemenson, P. I.; Underhill, A. E.; Kobayashi, A.; Kobayashi, H. *Polyhedron* **1990**, *9*, 2053−2059.
(40) Fun, H.-K.; Sivakumar, K.; Shan, B.-Z.; You, X.-Z. *Acta Crystallogr.* **1996**, *C52*, 1152−1154.
(41) Shan, B.-Z.; You, X.-Z.; Fun, H.-K.; Sivakumar, K. *Acta Crystallogr.* **1996**, *C52*, 3035−3037.
(42) Shan, B.-Z.; Zhang, X.-M.; You, X.-Z.; Fun, H.-K.; Sivakumar, K. *Acta Crystallogr.* **1996**, *C52*, 1148−1150.
(43) Allen, F. H.; Kennard, O.; Watson, D. G.; Brammer, L.; Orpen, A. G.; Taylor, R. In *International Tables of Crystallography*; Wilson, A. J. C., Ed.; Kluwer Academic Publishers: Boston, 1995; Sect. 9.5.
(44) Shupack, S. I.; Billig, E.; Clark, R. J. H.; Williams, R.; Gray, H. B. *J. Am. Chem. Soc.* **1964**, *86*, 4594−4602.
(45) Alavarez, S.; Vicente, R.; Hoffmann, R. *J. Am. Chem. Soc.* **1985**, *107*, 6253−6277 and references therein.
(46) Sano, M.; Adachi, H.; Yamatera, H. *Bull. Chem. Soc. Jpn.* **1981**, *54*, 2636−2641.
(47) Herman, Z. S.; Kirchner, R. F.; Loew, G. H.; Mueller-Westerhoff, U.; Nazzal, A.; Zerner, M. C. *Inorg. Chem.* **1982**, *21*, 46−56.
(48) Huyett, J. E.; Choudhury, S. B.; Eichhorn, D. M.; Bryngelson, P. A.; Maroney, M. J.; Hoffman, B. M. *Inorg. Chem.* **1998**, *37*, 1361−1367. Note that the coordinate system used in this work and in refs 53 and 54 reverses the positions of the *x*- and *y*-axes compared to those of the present system.
(49) Rosa, A.; Ricciardi, G.; Baerends, E. J. *Inorg. Chem.* **1998**, *37*, 1368−1379.
(50) Lauterbach, C.; Fabian, J. *Eur. J. Inorg. Chem.* **1999**, 1995−2004.
(51) Aragoni, M. C.; Arca, M.; Demartin, F.; Devillanova, F. A.; Garau, F.; Lelj, F.; Lippolis, V.; Verani, G. *J. Am. Chem. Soc.* **1999**, *121*, 7098−7107.

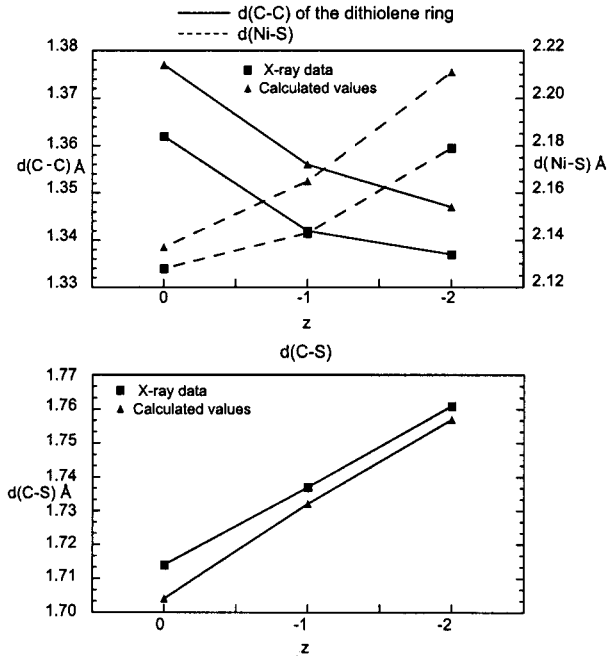

Figure 4. Experimental and theoretical values of bond lengths of the series $[Ni(S_2C_2Me_2)_2]^{0,1-,2-}$. Upper: C−C and Ni−S bonds. Lower: C−S bonds. The experimental esd's are comparable in size to the markers.

Table 3. Composition[a] of the Selected Orbitals of $[Ni(S_2C_2Me_2)_2]^z$

MO	z	Ni($3d_{xz}$)	Ni($3d_{yz}$)	Ni($4p_z$)	S($3p_z$)	C($2p_z$)	H(1s)
$5b_{2g}$	0	13.31			59.20	24.97	2.14
	1−	19.52			59.56	20.02	1.64
	2−	38.91			49.48	11.64	1.03
$6b_{1u}$	0			5.61	43.37	41.82	5.00
	1−			5.17	50.32	38.25	4.40
	2−			4.31	58.09	33.01	4.17
$4b_{3g}$	0		62.87		24.96	8.68	1.42
	1−		67.92		20.75	8.31	1.34
	2−		77.32		12.12	7.83	1.45

[a] Only contributions of more than 1.0% are taken into account; slight contributions of S(3d) (<2%) are not listed.

discrepancy in bond angle is 0.059° in the S−Ni−S angle of the neutral complex. As shown by the plots in Figure 4, experimental trends in Ni−S, C−S, and C−C bond lengths are reproduced by the calculations. Symmetries and relative energies of the frontier Kohn−Sham orbitals are set out in Figure 5. Compositions of selected orbitals are summarized in Table 3.

For the neutral complex, the HOMO is $6b_{1u}$, an orbital overwhelmingly ligand in character with only a small contribution from Ni($4p_z$) in all three oxidation states. The LUMO of the neutral complex is $5b_{2g}$, which becomes the SOMO in the monoanion and the HOMO in the dianion. A contour diagram of the $5b_{2g}$ orbital of the neutral complex, showing the section parallel to the molecular plane and 0.8 Å above it, is presented in Figure 6. It shows antibonding interactions between nickel and sulfur atoms and bonding interactions between carbon atoms of the chelate rings. This orbital is mainly S($3p_z$) in character but does contain a significant contribution from Ni($3d_{xz}$) which increases with reduction. The $5b_{2g}$ orbital is 20% metal in character in the monoanion and 39% metal in the dianion. Across the series, this orbital is well separated in energy from the lower block of three orbitals, in which there is some inversion in order. The $4b_{3g}$ orbital is largely composed of Ni($3d_{yz}$). The calculations predict the $^2B_{2g}$ ground state for $[Ni(S_2C_2Me_2)_2]^{1-}$, whose principal g-values are given in Table 4. In general, EPR parameters of $[Ni(S_2C_2R_2)_2]^{1-}$ are not strongly dependent on R.[22,52] Consequently, the $^2B_{2g}$ ground state firmly established for $[Ni(S_2C_2(CN)_2)_2]^{1-}$ from single-crystal EPR[53,54] and ENDOR and ESEEM studies[48] doubtless applies to $[Ni(S_2C_2Me_2)_2]^{1-}$.

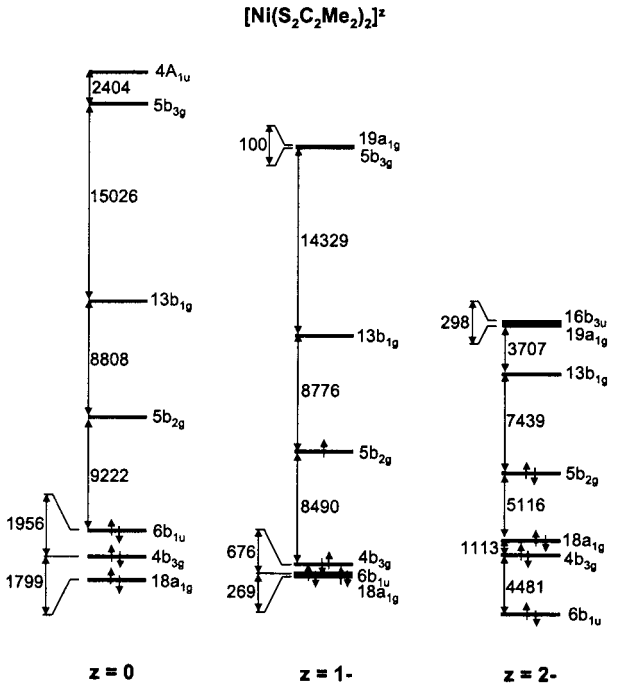

Figure 5. Energy level diagrams for members of the series $[Ni(S_2C_2Me_2)_2]^{0,1-,2-}$ obtained by DFT calculations. Orbital energy separations are given in inverse centimeters. For covenience in plotting, the energy levels of $[Ni(S_2C_2Me_2)_2]^{1-,2-}$ are shifted by −4.5 and −8.9 eV, respectively.

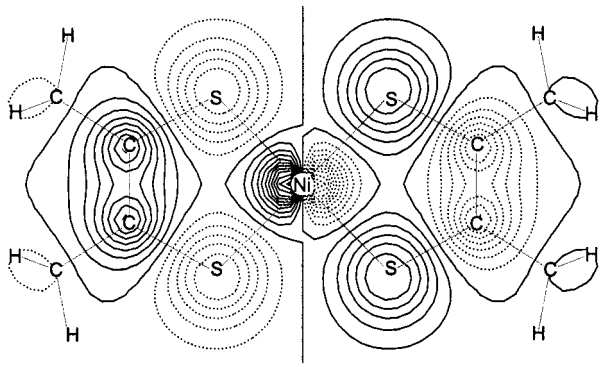

Figure 6. Contour plot of the $5b_{2g}$ orbital of $[Ni(S_2C_2Me_2)_2]$ showing the section parallel to the NiS_4 *xy*-plane and 0.8 Å above it.

Table 4. Experimental[a] and Calculated EPR Parameters for $[Ni(S_2C_2Me_2)_2]^{1-}$

	g_1	g_2	g_3
obs **g**-tensors	2.118	2.041	2.000
calc **g**-tensors	2.115	2.040	1.969

[a] In CH_2Cl_2/DMF (1:1 v/v) at 77 K.

Vibrational Frequencies. Values of Ni−S, C−S, and chelate ring C−C stretching frequencies for series **1** are collected in Table 5. Absorption frequencies for $[Ni(S_2C_2Me_2)_2]$ agree well

(52) Kirmse, R.; Stach, J.; Dietzsch, W.; Steimecke, G.; Hoyer, E. *Inorg. Chem.* **1980**, *19*, 2679−2685.
(53) Maki, A. H.; Edelstein, N.; Davison, A.; Holm, R. H. *J. Am. Chem. Soc.* **1964**, *86*, 4580−4587.
(54) Schmitt, R. D.; Maki, A. H. *J. Am. Chem. Soc.* **1968**, *90*, 2288−2292.

Table 5. Infrared Frequencies[a] for the Series $[Ni(S_2C_2Me_2)_2]^z$

z	C=C	C−S	Ni−S
0	1377, 1332	799, 565	465, 435
1−[b]	1508	768, 553	418[c]
2−[b]	1594	744, 543	[d]

[a] KBr, cm^{-1}. [b] Na^+ salts. [c] The second band was not measured (<400 cm^{-1}). [d] Not measured (<400 cm^{-1}).

with the previously reported values.[55] Assignments of the ν_{Ni-S}, ν_{C-S}, and ν_{C-C} are based on results of normal coordinate analysis of the infrared spectra of analogous complexes $[Ni(S_2C_2R_2)_2]^z$, where R = H, C_6H_5, CF_3, or CN and z = 0, 1−, or 2−.[56] Recently, Lauterbach and Fabian[50] reported an infrared spectrum calculated by DFT for $[Ni(S_2C_2H_2)_2]$, which is in good agreement with the experimental data and confirms assignments made by Schlapfer and Nakamoto.[56]

Values of ν_{Ni-S} and ν_{C-S} decrease, while values of ν_{C-C} increase with increased reduction. While these bands do not correspond to pure vibrations, the trends unequivocally indicate that the dithiolene ligands assume more enedithiolate character upon reduction. This behavior is in accord with the previously discussed changes of structural parameters.

Summary. The following are the principal results and conclusions of this investigation.

1. All members of the reversible electron-transfer series $[Ni(S_2C_2Me_2)_2]^{0,1-,2-}$ have been prepared and shown to have planar structures of idealized D_{2h} symmetry.

2. Across series **1**, a systematic trend in vibrational frequencies and bond lengths is apparent: ν_{C-C}, d(Ni−S), and d(S−C) increase, while ν_{Ni-S}, ν_{C-S}, and d(C−C) decrease. The trends indicate that in $[Ni(S_2C_2Me_2)_2]^{2-}$ the ligands approach an enedithiolate dianion state.

3. Geometry optimizations, performed at DFT level, reproduce X-ray structures of all members of the series to within 0.032 Å and 0.6°. Experimentally observed trends in changes of the d(Ni−S), d(S−C), and d(C−C) by passing from neutral to monoanionic and dianionic complexes are reproduced. The largest descrepancy between the experimental g-values of $[Ni(S_2C_2Me_2)_2]^{1-}$ and those calculated by DFT is 0.031.

4. DFT calculations on the members of series **1** identify the electroactive orbital as $5b_{2g}$, which is mainly S($3p_z$) for all members. This orbital is highly delocalized, and electron-transfer reactions are largely ligand-based events. However, unlike the case of the reversible series $[M(CO)_2(S_2C_2Me_2)_2]^{0,1-,2-}$ (M = Mo, W),[57] the metal contribution to this orbital is not constant across the electron-transfer series but increases upon reduction and reaches 39% for $[Ni(S_2C_2Me_2)_2]^{2-}$. The difference is likely due to the presence of carbonyl ligands, which accumulate electron density as the molecules are reduced. In the case of $[Ni(S_2C_2Me_2)_2]^{0,1-,2-}$, the first reduction apparently almost saturates the ligand electronic capacity. As a result, significant changes in the orbital composition must take place in order to accommodate a second electron. The four times larger decrease in d(C−C) and two times larger upshift in ν_{C-C} upon transition from $[Ni(S_2C_2Me_2)_2]$ to $[Ni(S_2C_2Me_2)_2]^{1-}$ than from $[Ni(S_2C_2Me_2)_2]^{1-}$ to $[Ni(S_2C_2Me_2)_2]^{2-}$ support this idea. If an oxidation state description were to be made for the highly delocalized series **1** (Table 3), the Ni(II) formulation is apposite to the dianion (Figure 1).

As noted at the outset, this work provides the first electronic descriptions of bis(dithiolene)nickel complexes over three oxidation states at strict parity of ligand. It complements earlier DFT calculations by Lauterbach and Fabian[50] on a broad series of neutral complexes $[M(X_2C_2H_2)_2]$ (M = Ni, Pd, Pt; X = O, NH, S, Se) directed toward an explication of electronic structures and electronic and vibrational spectra. Except for $[Ni(O_2C_2H_2)_2]$, spin-unrestricted DFT calculations by these authors predict a singlet ground state and an excited triplet state (biradical, Figure 1). The approximate singlet−triplet gap proposed is ∼40 kcal/mol (14 000 cm^{-1}). From spin-restricted DFT calculations, we obtain the value of 26 kcal/mol (9222 cm^{-1}) for the HOMO−LUMO gap of $[Ni(S_2C_2Me_2)_2]$ (Figure 5), and a preliminary test shows that this value holds in the case of spin-unrestricted calculations. This result suggests that a biradical state is not accessible at room temperature.

Acknowledgment. This research was supported by NSF Grant CHE 98-76457 and NIH Grant 28856. We thank Professor T. Ziegler (University of Calgary) for access to computational facilities and Dr. S. Patchkovskii (University of Calgary) for assistance with DFT calculations.

Supporting Information Available: X-ray crystallographic files in CIF format for the structure determinations of the three compounds in Table 1. This material is available free of charge via the Internet at http://pubs.acs.org.

IC010138Y

(55) Siimann, O.; Fresco, J. *Inorg. Chem.* **1971**, *10*, 297−302.
(56) Schlapfer, C. W.; Nakamoto, K. *Inorg. Chem.* **1975**, *14*, 1338−1344.
(57) Fomitchev, D. V.; Lim, B. S.; Holm, R. H. *Inorg. Chem.* **2001**, *40*, 645−654.